nature structural & molecular biology

Crystal structure of bet3 reveals a novel mechanism for Golgi localization of tethering factor TRAPP

Yeon-Gil Kim[1], Eun Ju Sohn[2], Jawon Seo[3], Kong-Joo Lee[3], Heung-Soo Lee[4], Inhwan Hwang[2], Malcolm Whiteway[5], Michael Sacher[6] & Byung-Ha Oh[1]

Transport protein particle (TRAPP) is a large multiprotein complex involved in endoplasmic reticulum–to–Golgi and intra-Golgi traffic. TRAPP specifically and persistently resides on Golgi membranes. Neither the mechanism of the subcellular localization nor the function of any of the individual TRAPP components is known. Here, the crystal structure of mouse Bet3p (bet3), a conserved TRAPP component, reveals a dimeric structure with hydrophobic channels. The channel entrances are located on a putative membrane-interacting surface that is distinctively flat, wide and decorated with positively charged residues. Charge-inversion mutations on the flat surface of the highly conserved yeast Bet3p led to conditional lethality, incorrect localization and membrane trafficking defects. A channel-blocking mutation led to similar defects. These data delineate a molecular mechanism of Golgi-specific targeting and anchoring of Bet3p involving the charged surface and insertion of a Golgi-specific hydrophobic moiety into the channels. This essential subunit could then direct other TRAPP components to the Golgi.

The maintenance of the proper protein and lipid content of intracellular organelles, mediated by vesicular carriers, is crucial for the survival of eukaryotic cells. Multiple factors have been implicated in ensuring the correct delivery of these vesicles to their appropriate compartments. One class of these factors is made up of the large, multisubunit tethering complexes found on distinct organelles[1,2]. Because these complexes may be involved in the initial stages of vesicle recognition[3], ensuring that the complexes themselves are delivered to the correct organelles is a critical cellular event. So far, it has not been known how these complexes or their subunits are directed to their respective membranes.

TRAPP is a large complex (~1,000 kDa) required for tethering endoplasmic reticulum (ER)-derived vesicles to Golgi membranes and for intra-Golgi traffic[4,5]. The complex was first identified in yeast and later in human cells[4,6,7]. The subunits are distributed into two functionally distinct complexes consisting of seven to ten proteins that are highly conserved in evolution[4,7]. The interactions between the TRAPP components seem to be quite strong, as the complex remains assembled after incubation in solutions containing up to 1 M NaCl[7]. The biochemical function of any of the constituent proteins is virtually unknown, although the TRAPP complex itself is a guanine nucleotide exchange factor for Ypt1p[8]. The function of TRAPP on the Golgi must be vital because (i) seven subunits of the complex are indispensable for the growth of yeast[7] (ii) mutations in the human ortholog of the essential yeast subunit Trs20p are responsible for the X-linked recessive skeletal disorder spondyloepiphyseal dysplasia tarda[9] and (iii) the complex stably localizes to Golgi membranes[10]. The ability of purified TRAPP to bind specifically to ER-derived transport vesicles[5] places this complex as one of the most upstream factors in determining specificity in ER-to-Golgi membrane traffic.

Bet3p is the most highly conserved protein among the TRAPP components[11]. In yeast, Bet3p resides exclusively and functions on Golgi membranes[4,10]. Because many Golgi proteins recycle through the ER[12], the persistent localization of Bet3p and TRAPP to the Golgi is believed to be important for its putative function as a landmark for incoming vesicle traffic[10]. The mechanism mediating the stable localization of the complex to the Golgi is unknown. Bet3p and other TRAPP subunits can be extracted from membranes by salt but not by the detergent Triton X-100 (ref. 7). Furthermore, none of the TRAPP components contains a membrane-spanning domain. Together, these observations suggest that the complex is anchored on membranes by electrostatic interactions or post-translational modifications.

A variety of proteins synthesized in the cytosol selectively translocate to membrane-bound compartments directed by a distinct set of landmark proteins and lipid molecules on the membranes. Short-lived activated small G proteins and phosphoinositides are the major mediators in the membrane translocation of cytosolic or peripheral membrane proteins through protein-protein and protein-phospholipid interactions[13,14]. Lipidation of proteins, such as S-palmitoylation, N-myristoylation and prenylation, is another major determinant resulting in membrane-anchoring of cytosolic proteins[15–17]. Although many examples of lipidation-mediated compartment-specific localization of cytosolic proteins are found in

[1]Center for Biomolecular Recognition and [2]Center for Plant Intracellular Trafficking, Department of Life Science and Division of Molecular and Life Sciences, Pohang University of Science and Technology, Pohang, Kyungbuk, 790-784, Korea. [3]Center for Cell Signaling Research, Division of Molecular Life Sciences and College of Pharmacy, Ewha Womans University, Seoul, 120-750, Korea. [4]Pohang Accelerator Laboratory, Pohang, Kyungbuk, 790-784, Korea. [5]Biotechnology Research Institute, 6100 Royalmount Avenue, Montreal, Quebec, Canada H4P 2R2. [6]Montreal Proteomics Network, 6100 Royalmount Avenue, Montreal, Quebec, Canada H4P 2R2. Correspondence should be addressed to B.-H.O. (bhoh@postech.ac.kr) or M.S. (michael.sacher@bri.nrc.ca).

Published online 19 December 2004; doi:10.1038/nsmb871

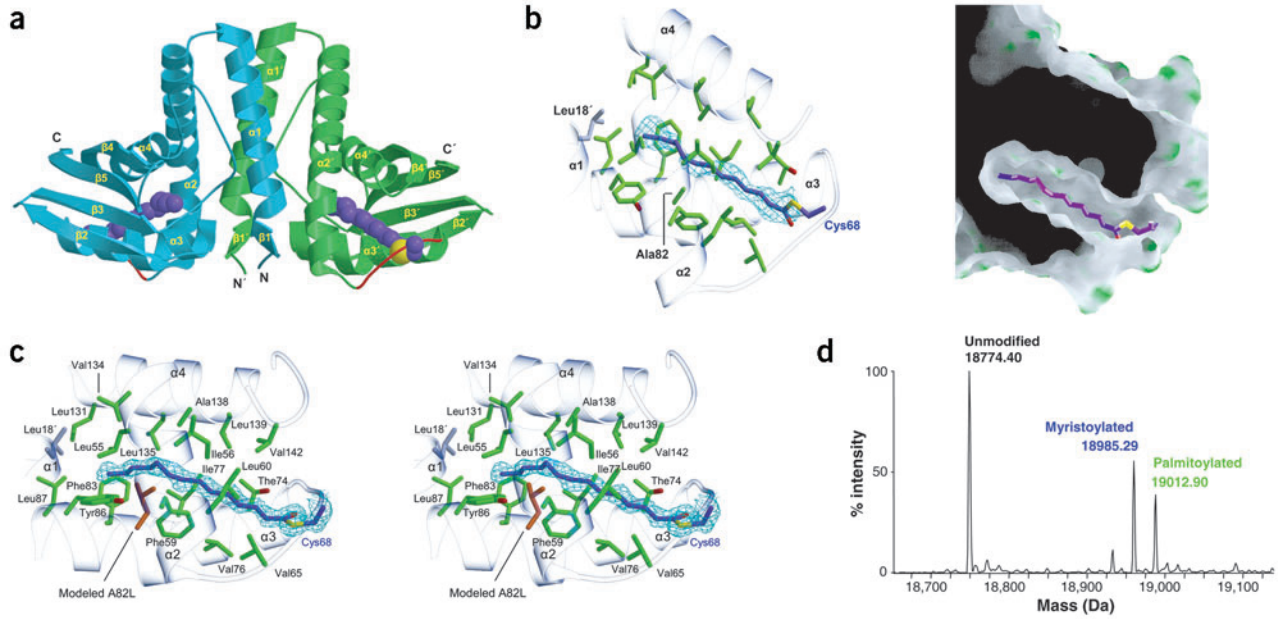

Figure 1 Overall structure, hydrophobic channel and S-acylation of bet3. (**a**) Dimeric structure. Myristoyl-Cys68 is a CPK model. The secondary structures are numbered in the order of appearance in the primary sequence. A portion of loop α2-α3, whose electron density was completely or partly missing, is red. (**b**) Myristoyl-Cys68 in the central hydrophobic channel. Left, the $F_o - F_c$ electron densities enclosed by the residues lining the channel, along with the final refined model of myristoyl-Cys68 in the structure of full-length bet3 (1.9 Å, 2.5 σ). The electron density map was calculated without myristoyl-Cys68. Cys68 was completely disordered, and its coordinates should be considered unfixed. Leu18 from the adjacent subunit is gray. Right, a cutaway view of the hydrophobic channel with the complete enclosure of the myristoyl-Cys68. An enlargement of the electron density around Cys68 is in **Supplementary Figure 1** online. (**c**) Stereo view of the hydrophobic channel in the structure of bet3(8–172). The $F_o - F_c$ electron density map (1.6 Å, 2.5 σ) was calculated with a model refined without myristoyl-Cys68. The side chain of Leu82 was modeled based on the coordinates of Ala82, which is conserved as alanine or glycine (**Fig. 3**). The modeling indicated that leucine at this position would not cause a steric hindrance with neighboring residues. (**d**) ESI mass spectrometric analysis of bet3(8–172) produced in *E. coli*. Deconvoluted mass spectrum shows unmodified, myristoylated (Δ210), and palmitoylated (Δ238) species. The unprocessed spectrum is in **Supplementary Figure 3** online.

the literature[18–20], the molecular mechanism underlying this process is still only vaguely understood[21–24].

Here, using the crystal structure of mouse bet3, we delineate a novel mechanism of how the bet3 subunit of TRAPP targets and localizes specifically to Golgi membranes, and propose a mechanism whereby this subunit is involved in the correct localization of the TRAPP complex to the Golgi.

RESULTS

Overall structure of bet3

The crystal structure of full-length mouse Bet3p (bet3) was solved with multiple MAD phasing using a crystal of selenomethionine (SeMet)-substituted protein. The final model, refined against data to a resolution of 1.9 Å, consists of residues 9–172. The structure is a mixed α/β fold containing four α-helices and five β-strands (**Fig. 1a**). A hairpin motif composed of β2 and β3 is juxtaposed with the other hairpin, composed of β4 and β5, forming an antiparallel β-sheet. One face of the sheet exhibits extensive hydrophobic interactions with α3 and α4. The other face of the sheet is exposed to the bulk solvent. The asymmetric unit of the crystal contained one molecule of bet3, which interacts extensively with a symmetry-related bet3 molecule. The intermolecular interaction is a typical pattern of domain swapping; β1 (residues 12–16) of one molecule is between β1 and α3 of the other molecule, whereas α1 of one molecule interacts with α2 of the other molecule (**Fig. 1a**). The dimer interface buries 1,921 Å^2 or 20.3% of the total monomeric surface, demonstrating that bet3 is a dimeric protein. This conclusion is supported by an immunoprecipitation study showing that Bet3p associates with Bet3p-protein A in a yeast strain expressing the two proteins[7]. Bet3p exhibits limited sequence homology with two other TRAPP components, Trs31p and Trs33p[7]. This observation suggests potential heteromeric interactions between Bet3p and either of these two proteins. We produced and purified recombinant mouse trs33 to homogeneity. However, we did not detect an interaction with bet3 as judged by both native gel electrophoresis and GST pull-down analyses in which one of the two components was present in substantial molar excess (data not shown). Nevertheless, large-scale yeast two-hybrid assays revealed interactions between Bet3p and Trs31p[25,26], leaving open the possibility of such hetero-oligomers in TRAPP. A database search for homologous structures in the Protein Data Bank revealed no protein with analogous folds.

A central hydrophobic channel and a distinctively flat surface

Complete chain tracing revealed that bet3 has a central hydrophobic channel defined by apolar side chains emanating from α2, α3 and α4 of one subunit and Leu18 on α1 of the other subunit (**Fig. 1b**). The channel is accessible from the entryway at one end, at which two completely disordered residues, Arg67 and Cys68, are located. Notably, the channel enclosed two closely juxtaposed elongated electron densities in the shape of a long alkyl chain. A myristate molecule could be fitted into the electron density. As the elongated electron densities were relatively weak, we suspected that an absolutely conserved residue, Cys68, might be acylated, but the flexibility of loop α2-α3 (residues 64–69) obscured the observation of the possible covalent bond formation. Crystals were obtained, however, from a truncated bet3

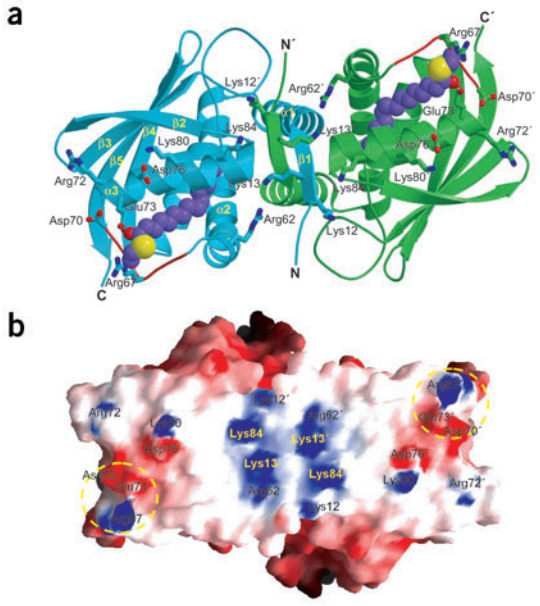

Figure 2 Unusually flat surface of bet3. (**a**) Ribbon drawing looking down the molecular two-fold axis, which runs perpendicular to the orientation of bet3 in **Figure 1a**. Myristoyl-Cys68 is a CPK model. The acidic or basic residues exposed on the surface are in ball-and-stick form. The flexible portion of loop α2-α3 is red. The coordinates of a completely disordered residue, Arg67, should be considered unfixed. (**b**) Electrostatic surface representation. The orientation of the molecule is the same as in **a**. The positive and negative charges arising from the indicated residues in **a** are in blue and red, respectively. Circles, positions of the entryway to the channel on each subunit. The two lysines substituted with glutamate (see text) are labeled with bold yellow letters.

(residues 8–172) in which loop α2-α3 is held in shape owing to the interaction of this loop with an adjacent molecule. As a consequence, a long and well-defined electron density connected to the sulfur atom of Cys68 was clearly observed (**Fig. 1c** and **Supplementary Fig. 1** online) and unequivocally identified as myristate on the basis of the high-resolution electron density map. Mass spectrometric analysis showed that the protein sample used for the crystallization was a mixture of three species (unmodified, myristoylated and palmitoylated bet3(8–172), **Fig. 1d**).

The myristoyl chain is completely enclosed by the hydrophobic residues lining the channel. Notably, the two channel entrances, related by molecular two-fold symmetry, are located at the edge of an unusually flat and wide surface of the bet3 dimer (**Fig. 2**). The surface is predominantly positively charged, having seven exposed basic residues per subunit, and therefore seems ideal for interacting with cell membranes. A multiple sequence alignment reveals that five (Lys13, Arg62, Arg67, Lys80 and Lys84) of the seven basic residues on the flat surface are >84% conserved (**Fig. 3**). Likewise, all of the residues lining the hydrophobic channel are virtually conserved (**Fig. 3**). The structural observations in conjunction with the sequence conservation pointed toward a mechanism of membrane-anchoring of bet3 involving both insertion of an acyl group within the hydrophobic channel and electrostatic interactions along the charged, flat surface.

Membrane-anchoring of Bet3p does not require S-acylation

Based on the structure of mouse bet3, we generated a mutant form of the protein containing the C68S substitution. Indeed, electron spray ionization (ESI) mass spectrometric analysis of the resulting protein indicated that the recombinant, mutated protein was not acylated (data not shown). Given the high degree of identity between bet3 orthologs (**Fig. 3**), we chose to examine the function of the structural features described above using the yeast model system. To examine whether Bet3p acylation was necessary for the function of the protein, we generated a yeast Bet3p mutant containing the substitution of the equivalent of mouse Cys68 with serine and a C-terminal HA-tag (Bet3p(C68S)-HA; mouse bet3 numbering is used throughout the text). Yeast cells expressing this mutant form of Bet3p as the sole copy of the protein were viable at all temperatures examined (**Table 1**), indicating that acylation of Bet3p is not critical for its function and that acylation of the recombinant protein was a serendipitous finding.

We next examined the subcellular localization of the HA-tagged wild-type and mutant constructs in yeast cells by both indirect immunofluorescence and gradient fractionation. Consistent with a previous report for Bet3p-GFP[10], the wild-type Bet3p-HA exhibited a punctate

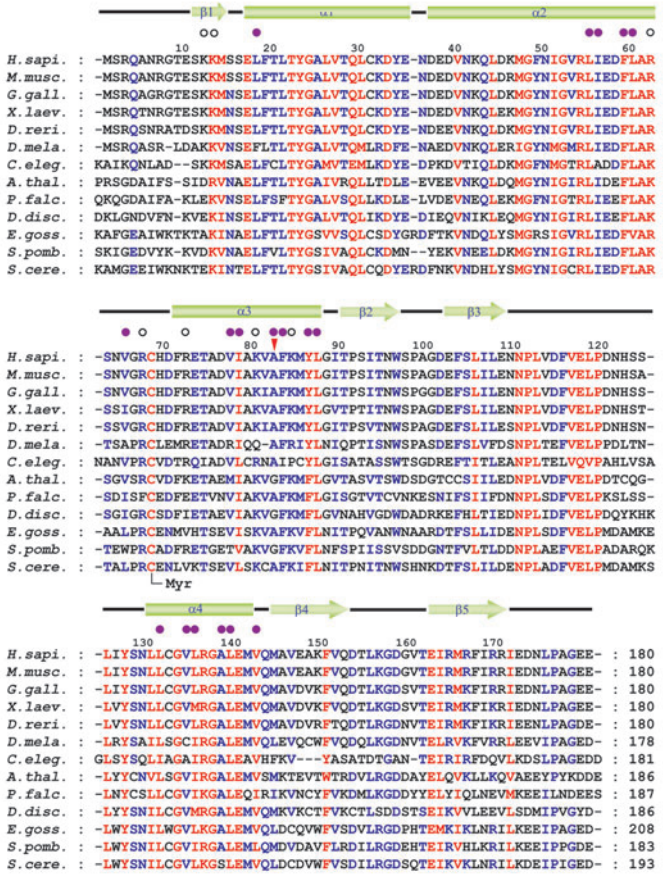

Figure 3 Secondary structure assignment and sequence alignment. The red and blue letters indicate the amino acids that are 100% and >80% conserved in 13 representative Bet3p orthologs available in public databases. Myr, the myristoyl group bound to Cys68 in the crystal. Filled circles, residues lining the wall of the hydrophobic channel. Red arrowhead, mutated residue used to limit the access of the fatty-acyl chain into the channel. Open circles, basic residues on the flat surface of the molecule. The secondary structure assignment at the top of the sequence shows that all of the insertions or deletions of amino acids are on loops. The accession codes for the Bet3p sequences are listed in the Methods.

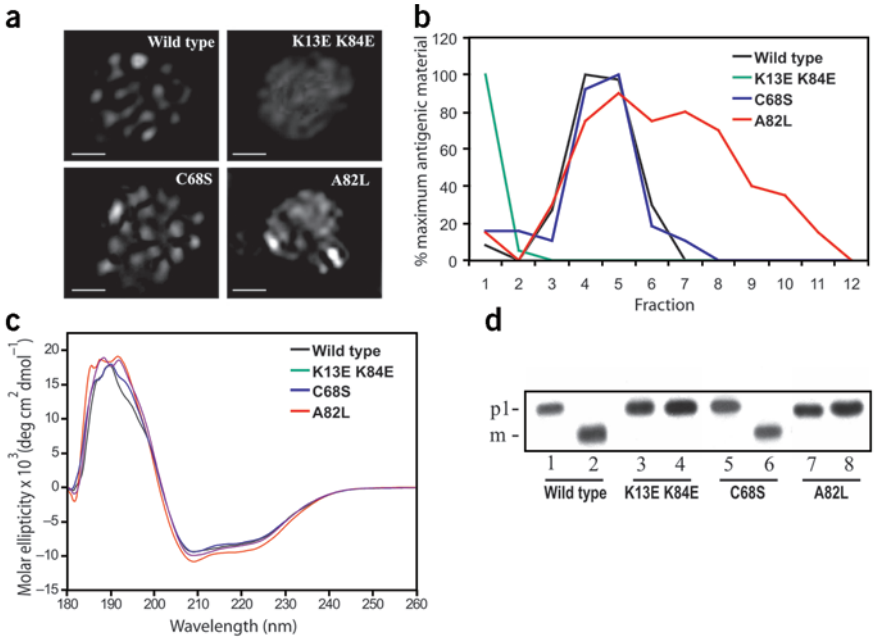

Figure 4 Phenotype of wild-type and mutant yeast Bet3p. (**a**) Indirect immunofluorescence. Yeast cells expressing either wild type, HA-tagged Bet3p (Bet3p-HA), or the mutants Bet3p(K13E K84E)-HA, Bet3p(C68S)-HA, and Bet3p(A82L)-HA were processed for indirect immunofluorescence as described in Methods. A representative cell at high magnification (100×) is shown in each panel. Scale bars, 1 μm. (**b**) Sucrose velocity gradient fractionation. Yeast cells expressing either Bet3p-HA or mutants were processed for sucrose velocity gradient fractionation as described in Methods. Fractions (1 ml) were collected from the top of the gradients and the Bet3 proteins were detected with anti-HA by western blot analysis. Cells in **a** and **b** were shifted to 37 °C for 1 h before the experiment. (**c**) CD spectroscopy. Overall structures of the recombinant wild-type mouse bet3 or the mouse mutant proteins were analyzed by CD spectroscopy as described in Methods. (**d**) Carboxypeptidase Y trafficking in wild-type and mutant Bet3p yeast cells. Yeast cells expressing either Bet3p-HA or mutants were shifted to 37 °C for 30 min before labeling with [^{35}S]methionine. Samples were then removed (lanes 1, 3, 5 and 7), unlabeled amino acid was added and the incubation was continued for 25 min (lanes 2, 4, 6 and 8). Carboxypeptidase Y was immunoprecipitated from lysates and detected by autoradiography. The positions of p1 (ER form) and m (vacuolar form) CPY are indicated at left.

staining pattern representing localization to the Golgi (**Fig. 4a**). The Bet3p(C68S)-HA also exhibited punctate staining nearly indistinguishable from that of wild type (**Fig. 4a**). We then examined Bet3p fractionation by sucrose velocity gradients. In the gradient system used, Golgi proteins including Bet3p have been shown to migrate in fractions 4–7 (refs. 10,27,28). Consistently, both Bet3p-HA and Bet3p(C68S)-HA peaked in these fractions (**Fig. 4b**, black and blue lines). These data therefore indicate that acylation of Bet3p is not necessary for its localization or function *in vivo*. Consistent with this notion, metabolic labeling of the yeast with tritiated palmitate or myristate did not reveal detectable levels of Bet3p acylation (data not shown).

Golgi targeting of Bet3p requires an open hydrophobic channel

As acylation of Bet3p was not needed for the function of the protein, we next examined the role of the hydrophobic channel. The fact that the recombinant protein was acylated was probably a serendipitous finding indicating that the channel could accommodate an acyl group. Therefore, we sought to block the channel by site-directed mutagenesis and examine the effects *in vivo*. A modeling experiment indicated that substitution of Ala82, a conserved residue located in the middle of the channel (**Fig. 1c**), with leucine seemed to have no effect on the local structure around the residue (**Fig. 4c** and data not shown), but would block access to most of the channel. In terms of a fatty-acyl chain, this mutant would allow accommodation of only the terminal six-carbon segment into the channel owing to steric hindrance. This mutation (A82L) was conditionally lethal (**Table 1**) and all experiments with it were done by preshifting the cells to 37 °C before analysis. Unlike the wild type and the C68S mutant, indirect immunofluorescence of Bet3p(A82L)-HA exhibited a nondescript pattern suggesting localization to a variety of intracellular compartments in the cell (**Fig. 4a**). Sucrose velocity gradient fractionation showed a wide distribution of this mutant protein throughout the gradient compared with wild-type Bet3p-HA (**Fig. 4b**, red line), again suggesting that the protein is found on multiple membranes. Although we did not detect acylation of Bet3p *in vivo*, one interpretation of the A82L phenotype is that if Bet3p were acylated, a substantial portion of the fatty-acyl chain from residue Cys68 would be exposed in the cytosol owing to the channel-blocking mutation. This would in turn drive nonspecific interactions of the mutant with membranes of various organelles or other hydrophobic molecules. Alternatively, because acylation of Cys68 is not essential, a Golgi-specific hydrophobic moiety may not have access to the Bet3p channels, resulting in association of this protein with numerous membranes via a nonselective process.

To distinguish between these two possibilities, we constructed the double mutant Bet3p(C68S A82L)-HA, in which the acylated cysteine residue was changed to a serine and the hydrophobic channel was blocked. If the phenotype of the Bet3p(A82L)-HA mutant yeast were due to acylated Bet3p's inability to sequester the acyl group, then the double mutant should behave as the Bet3p(C68S)-HA mutant and suppress the temperature-sensitive growth of the single Bet3p(A82L)-HA mutation. If, however, the Bet3p(A82L)-HA mutation were blocking access to a hydrophobic moiety from the Golgi (either from a protein or lipid), then the double mutant should behave like the Bet3p(A82L)-HA mutant. The Bet3p(C68S A82L)-HA double mutant behaved as the Bet3p(A82L)-HA mutant (**Table 1**). This result indicates that the conditional lethality of the Bet3p(A82L)-HA mutant was not due to acylation of Bet3p and suggests that Bet3p requires an open hydrophobic channel, for insertion of an acyl group from another molecule, to properly localize to Golgi membranes.

Table 1 Summary of yeast Bet3p mutations

Mutation	Phenotype[a]
K13E K84E	ts
C68S	ND
A82L	ts
C68S A82L	ts

Growth was tested on YPD medium. ts, temperature-sensitive for growth at 37 °C. ND, no detectable growth defects.

[a]All genes were expressed under the endogenous *BET3* promoter.

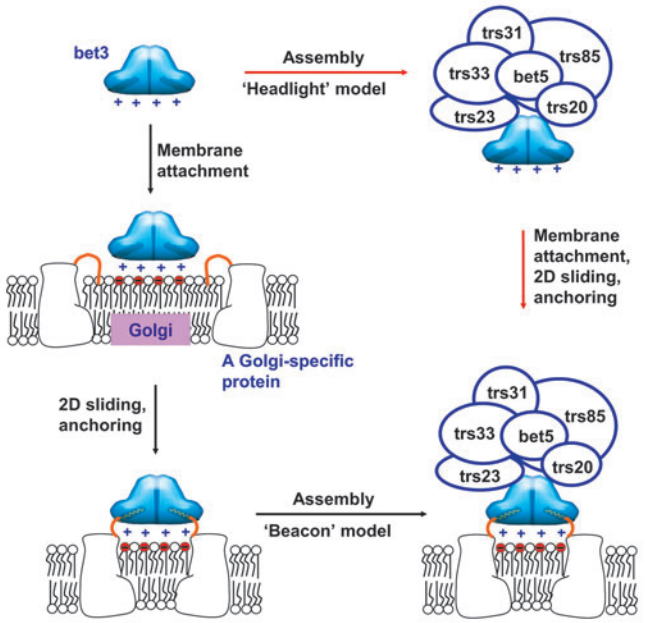

Figure 5 Model for Golgi-specific targeting and localization of TRAPP. The flat surface of mouse bet3, which is predominantly positively charged, would interact with negatively charged polar head groups of lipids. The landed bet3 protein could search for its Golgi-specific partner protein in a two-dimensional fashion. The secondary and firm attachment of bet3 to the Golgi occurs via the insertion of the acyl chain of the partner protein into the hydrophobic channel of bet3. In the beacon model, bet3 first attaches to the Golgi and directs the recruitment of the other TRAPP subunits. In the headlight model, the complex or a portion of the complex is preassembled in the cytosol and directed to the Golgi by the bet3 subunit. Secondary attachment to the Golgi would occur via the acyl groups as described above. The schematic drawing of the TRAPP complex does not reflect how TRAPP components interact with each other in the complex, which is as yet unknown.

The surface of Bet3p is crucial for Golgi-specific targeting

Because the channel-blocked mutant (Bet3p(A82L)-HA) was found on multiple compartments in the yeast cell, we speculated that there must be another, less specific way to bring the subunit to the membranes. We therefore focused our attention on the flat, positively charged surface of bet3, which is adjacent to the entrances to the hydrophobic channels. Of the highly conserved basic residues exposed on the flat surface (**Fig. 3**), we doubly substituted Lys13 and Lys84 with glutamate and examined the localization of the charge-inversion mutant (Bet3p(K13E K84E)-HA). This mutation was conditionally lethal (**Table 1**) and all experiments with it were done by preshifting the cells to 37 °C before analysis. The Bet3p(K13E K84E)-HA mutant gave a diffuse pattern with weak punctate stains (**Fig. 4a**), suggesting that this mutated protein is soluble. Sucrose velocity gradient fractionation of this mutant showed that virtually all of the mutant protein was detected in the soluble fraction (**Fig. 4b**, green line, fraction 1). Taken together, the data indicate that the charge-inversion mutant could no longer be targeted to the membranes. Therefore, the flat surface with the prominent positive electrostatic nature is indeed important for membrane recognition and seems to function upstream of the hydrophobic channel to mediate Golgi-specific localization of bet3.

To rule out the possibility that the introduced mutations perturbed the structural integrity of the protein, we expressed and purified recombinant yeast and mouse Bet3p and the mutants from *Escherichia coli* and analyzed them by several biophysical methods. Wild-type and mutant mouse bet3 proteins exhibited unaltered biophysical properties as analyzed by analytical ultracentrifugation, size-exclusion chromatography or circular dichroism (CD) spectroscopy (**Fig. 4c** and data not shown). In all cases, the proteins behaved as dimers with identical secondary structures. Owing to poor expression, solubility and instability, we could only record the CD spectra for wild type, Bet3p(C68S) and Bet3p(K13E K84E) from yeast that were virtually identical to each other (**Supplementary Methods** and **Supplementary Fig. 2** online). These results, together with the high degree of identity between yeast and mouse bet3, suggest that the observed phenotypes of the mutants used in this study are not attributable to a change in the overall structure of the resulting proteins.

Mislocalization of Bet3p affects ER-to-Golgi transport

We next investigated the effect of the expression of the mutants on the intracellular trafficking of the marker protein carboxypeptidase Y (CPY). During pulse-chase experiments, CPY can be found in several forms including a p1 (ER) form, a p2 (Golgi) form and the mature vacuolar form[29]. Trafficking of CPY in yeast cells expressing either Bet3p-HA, Bet3p(C68S)-HA, Bet3p(K13E K84E)-HA or Bet3p(A82L)-HA was assayed by pulse-chase analysis. All strains exhibited the p1 form of CPY after the pulse (**Fig. 4d**, lanes 1, 3, 5 and 7). After the chase, only Bet3p-HA and Bet3p(C68S)-HA could process p1 CPY to the mature form (**Fig. 4d**, lanes 2 and 6). Both Bet3p(K13E K84E)-HA and Bet3p(A82L)-HA showed a block in ER-to-Golgi traffic as only the p1 form of CPY was seen after the chase (**Fig. 4d**, lanes 4 and 8). Therefore, each of the yeast Bet3p mutations that affect membrane localization of this subunit also show a block in CPY trafficking at the ER-Golgi level.

DISCUSSION

We have presented the first study addressing how a component of a tethering complex involved in intracellular transport is localized to a specific cellular organelle. The main mechanism driving Bet3p to the membranes involves the large, flat, charged surface found on the bet3 protein. In particular, Lys13 and Lys84 in mouse bet3 seem critical for this process. Once bound to the membranes, a hydrophobic moiety could then insert into the hydrophobic channels of the bet3 dimer, thus anchoring the protein to the membranes. The hydrophobic moiety is probably a hydrocarbon chain of a lipid molecule rather than a protein side chain, considering the narrow and deep dimension of the hydrophobic channel. We speculate that this hydrophobic moiety must be enriched on Golgi membranes to impart Golgi-specific localization of bet3. This notion is supported by the fact that, when access to the hydrophobic channels is blocked, bet3 can associate with multiple intracellular membranes. In this way, bet3 could 'sample' the membranes and would be stably anchored only to the membrane containing the hydrophobic moiety to be inserted into the channels.

Notably, although Cys68 is 100% conserved over all known bet3 orthologs, we found that this residue was not essential for Bet3p structure or function under the laboratory conditions used in this study. Convincing proof of this was provided by the identical phenotypes between wild type and the Bet3p(C68S) mutant (**Fig. 4**). This is in contrast to the acyl group on the catalytic subunit of cAMP-dependent protein kinase, which influences protein structure[30]. It is possible that conservation of the cysteine residue proximal to a hydrophobic channel may be necessary under different conditions. We believe that acylation of bet3 is merely opportunistic, because the cysteine residue is located near a channel that can accommodate a acyl group with high transfer potential, such as myristoyl-CoA, and because the protein is heterogeneously

Table 2 Data collection, phasing and refinement statistics

	bet3 (full-length)	SeMet-bet3 (full-length)			bet3 (8–172)
Data collection					
Space group	$P4_32_12$	$P4_32_12$			$P3_121$
Cell dimensions (Å)					
a	54.25	54.37			72.73
b	54.25	54.37			72.73
c	113.76	109.77			56.56
		peak	*inflection*	*remote*	
Wavelength	1.5418	0.97928	0.97942	0.97175	1.5418
Resolution (Å)		30.0–2.7	30.0–2.7	30.0–2.7	
R_{sym}[a]		3.3 (14.8)	3.0 (13.9)	2.7 (14.7)	
$I / \sigma I$[a]		29.8 (3.8)	32.7 (4.3)	36.3 (4.5)	
Completeness (%)[a]		93.1 (86.2)	93.6 (87.4)	94.5 (90.1)	
Redundancy		8.5	9.4	10.6	
Refinement					
Resolution (Å)	30.0–1.9				30.0–1.6
No. reflections[b]	141,514				200,289
R_{work} / R_{free}	21.7 / 26.0				20.6 / 22.4
No. atoms					
Protein	1,288				1,272
Water	67				134
B-factors					
Protein	34.02				16.93
Water	41.87				27.96
R.m.s. deviations					
Bond lengths (Å)	0.0134				0.00548
Bond angles (°)	1.5958				1.13873

[a]Values in parentheses are for the highest resolution shell. [b]Reflections of $|F_{obs}| > 1.0\ \sigma$.

acylated in *E. coli*. If it exists at all, the acylated protein may represent only a small proportion in eukaryotic cells. In this case, we speculate that acylated Bet3p would be nonfunctional because the channel would be inaccessible to other hydrophobic moieties.

Two models for the Golgi-specific targeting and localization of mammalian TRAPP via the bet3 subunit based on the presented data can be envisioned (**Fig. 5**). In one model, which we refer to as the 'headlight' model, bet3, as part of an assembled mammalian TRAPP complex, could search for and recognize organelles in a nonspecific fashion through an electrostatic interaction between the unique surface and negatively charged head groups in the membranes. Once in contact with the Golgi, the bet3 protein searches for the putative partner protein, which carries a post-translationally modified fatty acyl chain. We assume that this hydrophobic moiety is not properly sequestered in a hydrophobic environment, and the channel on the bet3 protein provides an energetically favorable hiding place to drive the binding of the two, resulting in the tight anchoring of this TRAPP subunit to the Golgi. According to this model, the putative partner protein would be a Golgi-specific protein that is not extractable from the membranes by a salt wash. If the bet3 protein failed to be anchored owing to association with another organelle, the protein would eventually be released and free to search for the correct compartment. In this process, the flexibility of loop α2-α3 may serve several purposes. The loop could (i) be involved in binding to the putative Golgi-specific partner, thus bringing the acyl chain in close proximity to the hydrophobic channel; and/or (ii) be involved in shielding the channel from the polar environment. Although it is possible that the charged surface of bet3 interacts with a negatively charged surface on a protein, we do not favor this possibility, because the A82L mutant was capable of interacting with multiple organelles, suggesting that such an interacting protein would be distributed over a wide array of membranes. Such a scenario would then compete bet3 away from the Golgi, where it is needed for its function[4]. In the second model, referred to as the 'beacon' model, bet3 is first anchored by itself or with a subset of TRAPP subunits to the Golgi in a similar manner to the headlight model. The bet3 protein would then serve as a landmark responsible for the Golgi-specific recruitment of some or all of the other mammalian TRAPP components. In this model, bet3 would function analogously to how Sec3p has been proposed to function for the exocyst tethering factor in yeast[31]. The two models are not mutually exclusive and bet3 could bind to membranes both with and without other TRAPP subunits.

The described process should be conserved throughout all eukaryotes, because TRAPP components, especially Bet3p, share unusually high sequence homologies throughout evolution. This is supported by the marked correlation between the structure of mouse bet3 protein and the function of yeast Bet3p probed by the mutagenesis study presented here. It is formally possible that the bet3 mutations affect the assembly of the complex, thus indirectly affecting membrane attachment. However, the differential behavior seen with the Bet3p(A82L) and Bet3p(K13E K84E) mutants would argue strongly in favor of a direct interaction between bet3 and membranes. In addition, such an alternative explanation would necessitate acylation of another TRAPP subunit for insertion of the lipid into the bet3 channel, which is not supported by metabolic labeling of yeast with tritiated palmitate or myristate (data not shown). Thus the simplest interpretation consistent with all of our data is that the mutations directly affect bet3-membrane interactions.

Another class of proteins whose lipid groups are found in differing microenvironments are the rab GTPases. Prenyl groups on these proteins are sequestered by either rab GDP dissociation inhibitor (rab-GDI) or rab escort protein, both of which appear to have a deep cavity or a binding groove to accommodate the geranylgeranyl moieties[32]. With the isoprenoid-binding cavity, rab-GDI can extract the membrane-inserted isoprenoids to solubilize rab proteins. In the proposed models, bet3 accepts an improperly sequestered acyl group from a Golgi-bound protein and then is stably anchored on the Golgi. This acyl group could be found in several possible places before insertion into the hydrophobic channel of bet3. The acyl group could be partially buried within the lipid bilayer, and bet3, like rab-GDI, could extract the lipid and sequester it in the hydrophobic channel. An alternative possibility is that acylation of the Golgi-localized protein occurs in response to TRAPP binding to the Golgi membranes. This might be mediated by the TRAPP subunit Trs20p/sedlin, whose structure reveals similarities to the N-terminal portion of the SNARE protein Ykt6p[33]. Recently, Ykt6p has been shown to mediate the nonenzymatic acylation of the protein Vac8p before vacuolar fusion[34]. Taken together, bet3 binding to Golgi membranes may be coupled to Trs20p-mediated acylation of the putative Golgi-localized protein, thus coordinating membrane recognition with stable attachment to the Golgi.

In conclusion, we have delineated a novel mechanism for Golgi-specific recruitment of the Bet3p subunit of the tethering factor TRAPP through two unusual structural features: a flat and positively charged

surface that is likely to recognize membranes in a self-sufficient manner and a hydrophobic channel capable of sequestering a fatty-acyl chain. We have also presented models whereby this subunit could direct the localization of all or some of the other TRAPP components. The mutants generated in this study are now being used in yeast genetic screens to identify other components responsible for Golgi-specific localization of this complex.

METHODS

Protein expression and purification of bet3. The bet3 gene was amplified by PCR from a mouse lung cDNA library (Stratagene) and ligated into the pGEX-4T3 vector. bet3 was produced in *E. coli* BL21 (DE3) strain as a fusion protein containing glutathione *S*-transferase (GST) at the N terminus. Bacterial lysates were prepared by sonication in buffer A consisting of 50 mM Tris-HCl, pH 8.0, 100 mM NaCl, and 1 mM DTT. The protein bound to GST-bind resin (Novagen) was eluted with buffer A containing 10 mM glutathione. The eluted solution was reacted with thrombin (Roche Molecular Biochemicals) for 5 h at 24 °C and loaded onto a Resource Q column (Amersham Biosciences). bet3 was eluted with a 0–500 mM linear NaCl gradient in buffer A. The protein was further purified using a HiLoad 26/60 Superdex 200 gel-filtration column (Amersham Biosciences). bet3(8–172) was purified according to the same procedure described above.

Crystallization and structure determination. Crystals of bet3 and bet3(8–172) were obtained by hanging-drop vapor diffusion at 24 °C by mixing and equilibrating 2 μl of each of the protein solutions with a precipitant solution. The precipitant for bet3 contained 28% (v/v) PEG 600, 5% (w/v) PEG 1000, 10% (v/v) glycerol, and 0.1 M MES, pH 5.8. That for bet3(8–172) contained 28% (w/v) PEG monomethyl ether 2000, 0.2 M ammonium sulfate, and 0.1 M sodium acetate, pH 4.5. A MAD data set was collected with a crystal of SeMet-substituted bet3 on beamline 6B of the Pohang Accelerator Laboratory. Phase determination and improvement were carried out with SOLVE[35] and RESOLVE[36], respectively. Model building and refinement were done with O[37] and CNS[38], respectively. The native diffraction data for both bet3 and bet3(8–172) crystals were collected with a Raxis IV^{++} area detector system on a Ultrix-18 X-ray generator (Rigaku). All diffraction data were processed using DENZO and SCALEPACK[39]. The crystals of both bet3 and bet3(8–172) contained one protein molecule in the asymmetric unit. The structure of bet3(8–172) was determined by molecular replacement with the CCP4 version of AmoRe[40] using the structure of bet3. Crystallographic data statistics are summarized in **Table 2**.

Construction of plasmids and yeast transformation. The *BET3* gene was obtained from yeast genomic DNA by PCR. All the mutant Bet3p genes were created by two sequential PCR reactions and confirmed by sequencing. The PCR products were cloned into pBluescript (KS+) (Stratagene) to produce the proteins with an HA-tag at the C terminus. Each of the genes was transferred to pVT-U, a yeast expression vector using the *ADH* promoter with a *URA3* selection marker. The resulting plasmids were then digested with BglII and either SmaI (for wild type and K13E K84E mutant) or XhoI followed by blunt-end repair of the XhoI site (for C68S and A82L mutants). The ~600-bp fragments were inserted into pRS315 (*CEN*, *LEU2*) containing the *BET3* ORF with upstream and downstream untranslated elements by first removing most of the ORF with BglII and SnaBI and ligating the tagged constructs into the resulting BglII and blunt sites. Yeast cells (*MATa/α ura3/ura3 leu2/leu2 BET3/bet3:URA3*) were then transformed with each of the plasmids. Transformants were selected on SD-Leu plates, sporulated and dissected. *LEU*$^+$*URA*$^+$ colonies, in which the sole copy of *BET3* originates from the plasmid, were used in the experiments described.

Indirect immunofluorescence, CPY trafficking and sucrose gradient fractionation. Standard methods were used for these procedures and are described in detail[5,10]. Antibodies used for these procedures were: anti-HA (Covance, 1:2,000), goat anti-mouse-CY3 (Jackson Immunoresearch, 1:1,000), anti-mouse-HRP (Santa Cruz Biotechnology, 1:5,000) and anti-CPY (gift from T. Stevens, University of Oregon).

CD spectroscopy. Data were collected on a Jasco J-715 spectropolarimeter at 25 °C in a cuvette with 3-mm path length. CD spectra were recorded with protein samples (2.7 μM) in 5 mM phosphate buffer, pH 7.5, over a range of 180–260 nm in a nitrogen atmosphere. Each spectrum is the accumulation of three scans corrected by subtracting signals from the buffer control.

Sequence alignment and accession codes. Sequences of 13 Bet3p orthologs available in public databases were aligned using ClustalW[41] (**Fig. 3**). The GenBank accession numbers for the Bet3p sequences are *H. sapi.* (*Homo sapiens*, NP_055223), *M. musc.* (*Mus musculus*, AAH03736), *G. gall.* (*Gallus gallus*, XP_417772), *X. laev.* (*Xenopus laevis*, AAH53802), *D. reri.* (*Dario rerio*, AAH78259), *D. mela.* (*Drosophila melanogaster*, AAF50270), *C. eleg.* (*Caenorhabditis elegans*, NP_499100), *A. thal.* (*Arabidopsis thaliana*, NP_200286), *P. falc.* (*Plasmodium falciparum*, NP_702835), *D. disc.* (*Dictyostelium discoideum*, AAO51174), *E. goss.* (*Eremothecium gossypii*, AA54790), *S. pomb.* (*Scizosaccharomyces pombe*, NP_593886) and *S. cere.* (*Saccharomyces cerevisiae*, NP_012994).

Coordinates. The coordinates of the bet3 and bet3(8–172) structures have been deposited in the Protein Data Bank (accession codes 1WC8 and 1WC9, respectively).

ACKNOWLEDGMENTS

We are grateful to M. Cygler (Biotechnology Research Institute) for invaluable input and discussions on this work, J. Wagner for technical assistance, and T. Stevens (University of Oregon) and S. Ferro-Novick (Yale University) for providing strains and reagents. This study made use of beamline 6B at Pohang Accelerator Laboratory. This work was supported by Creative Research Initiatives of the Korean Ministry of Science & Technology and by the Réseau Protéomique de Montréal Proteomics Network. Y.-G.K. was supported by the Brain Korea 21 Project.

COMPETING INTERESTS STATEMENT

The authors declare that they have no competing financial interests.

Note: Supplementary information is available on the Nature Structural & Molecular Biology website.

Received 13 September; accepted 17 November 2004
Published online at http://www.nature.com/nsmb/

1. Guo, W., Sacher, M., Barrowman, J., Ferro-Novick, S. & Novick, P. Protein complexes in transport vesicle targeting. *Trends Cell Biol.* **10**, 251–255 (2000).
2. Whyte, J.R. & Munro, S. Vesicle tethering complexes in membrane traffic. *J. Cell Sci.* **115**, 2627–2637 (2002).
3. Lee, M.C.S., Miller, E.A., Goldberg, J., Orci, L. & Schekman, R. Bi-directional protein transport between the ER and Golgi. *Annu. Rev. Cell Dev. Biol.* **20**, 87–123 (2004).
4. Sacher, M. *et al.* TRAPP, a highly conserved novel complex on the *cis*-Golgi that mediates vesicle docking and fusion. *EMBO J.* **17**, 2494–503 (1998).
5. Sacher, M. *et al.* TRAPP I implicated in the specificity of tethering in ER-to-Golgi transport. *Mol. Cell* **7**, 433–442 (2001).
6. Gavin, A.C. *et al.* Functional organization of the yeast proteome by systematic analysis of protein complexes. *Nature* **415**, 141–147 (2002).
7. Sacher, M., Barrowman, J., Schieltz, D., Yates, J.R. 3rd & Ferro-Novick, S. Identification and characterization of five new subunits of TRAPP. *Eur. J. Cell Biol.* **79**, 71–80 (2000).
8. Wang, W., Sacher, M. & Ferro-Novick, S. TRAPP stimulates guanine nucleotide exchange on Ypt1p. *J. Cell Biol.* **151**, 289–296 (2000).
9. Gedeon, A.K. *et al.* Identification of the gene (SEDL) causing X-linked spondyloepiphyseal dysplasia tarda. *Nat. Genet.* **22**, 400–404 (1999).
10. Barrowman, J., Sacher, M. & Ferro-Novick, S. TRAPP stably associates with the Golgi and is required for vesicle docking. *EMBO J.* **19**, 862–869 (2000).
11. Rossi, G., Kolstad, K., Stone, S., Palluault, F. & Ferro-Novick, S. BET3 encodes a novel hydrophilic protein that acts in conjunction with yeast SNAREs. *Mol. Biol. Cell* **6**, 1769–1780 (1995).
12. Cole, N.B., Ellenberg, J., Song, J., DiEuliis, D. & Lippincott-Schwartz, J. Retrograde transport of Golgi-localized proteins to the ER. *J. Cell Biol.* **140**, 1–15 (1998).
13. Munro, S. Organelle identity and the targeting of peripheral membrane proteins. *Curr. Opin. Cell Biol.* **14**, 506–514 (2002).
14. Lemmon, M.A. Phosphoinositide recognition domains. *Traffic* **4**, 201–213 (2003).
15. Bijlmakers, M.J. & Marsh, M. The on-off story of protein palmitoylation. *Trends Cell Biol.* **13**, 32–42 (2003).
16. Liu, J., Hughes, T.E. & Sessa, W.C. The first 35 amino acids and fatty acylation sites determine the molecular targeting of endothelial nitric oxide synthase into the Golgi region of cells: a green fluorescent protein study. *J. Cell. Biol.* **137**, 1525–1535 (1997).
17. Shenoy-Scaria, A.M., Dietzen, D.J., Kwong, J., Link, D.C. & Lublin, D.M. Cysteine3 of Src family protein tyrosine kinase determines palmitoylation and localization in caveolae. *J. Cell Biol.* **126**, 353–363 (1994).
18. Murray, D. *et al.* Electrostatics and the membrane association of Src: theory and experiment. *Biochemistry* **37**, 2145–2159 (1998).
19. Brennwald, P. & Novick, P. Interactions of three domains distinguishing the Ras-related GTP-binding proteins Ypt1 and Sec4. *Nature* **362**, 560–563 (1993).

20. Zhou, W. & Resh, M.D. Differential membrane binding of the human immunodeficiency virus type 1 matrix protein. *J. Virol.* **70**, 8540–8548 (1996).
21. McCabe, J.B. & Berthiaume, L.G. Functional roles for fatty acylated amino-terminal domains in subcellular localization. *Mol. Biol. Cell* **10**, 3771–3786 (1999).
22. Resh, M.D. Fatty acylation of proteins: new insights into membrane targeting of myristoylated and palmitoylated proteins. *Biochim. Biophys. Acta* **1451**, 1–16 (1999).
23. Pfeffer, S.R. Rab GTPases: specifying and deciphering organelle identity and function. *Trends Cell Biol.* **11**, 487–491 (2001).
24. Sivars, U., Aivazian, D. & Pfeffer, S.R. Yip3 catalyses the dissociation of endosomal Rab–GDI complexes. *Nature* **425**, 856–859 (2003).
25. Uetz, P. *et al.* A comprehensive analysis of protein-protein interactions in Saccharomyces cerevisiae. *Nature* **403**, 623–627 (2000).
26. Ito, T. *et al.* Toward a protein-protein interaction map of the budding yeast: A comprehensive system to examine two-hybrid interactions in all possible combinations between the yeast proteins. *Proc. Natl. Acad. Sci. USA* **97**, 1143–1147 (2000).
27. Schroder, S., Schimmoller, F., Singer-Kruger, B. & Riezman, H. The Golgi-localization of yeast Emp47p depends on its di-lysine motif but is not affected by the ret1-1 mutation in α-COP. *J. Cell Biol.* **131**, 895–912 (1995).
28. Otte, S. *et al.* Erv41p and Erv46p: new components of COPII vesicles involved in transport between the ER and Golgi complex. *J. Cell Biol.* **152**, 503–518 (2001).
29. Stevens, T., Esmon, B. & Schekman, R. Early stages in the yeast secretory pathway are required for transport of carboxypeptidase Y to the vacuole. *Cell* **30**, 439–448 (1982).
30. Tholey, A., Pipkorn, R., Bossemeyer, D., Kinzel, V. & Reed, J. Influence of myristoylation, phosphorylation, and deamidation on the structural behavior of the N-terminus of the catalytic subunit of cAMP-dependent protein kinase. *Biochemistry* **40**, 225–231 (2001).
31. Finger, F.P., Hughes, T.E. & Novick, P. Sec3p is a spatial landmark for polarized secretion in budding yeast. *Cell* **92**, 559–571. (1998).
32. Rak, A. *et al.* Structure of Rab GDP-dissociation inhibitor in complex with prenylated YPT1 GTPase. *Science* **302**, 646–650 (2003).
33. Jang, S.B. *et al.* Crystal structure of SEDL and its implications for a genetic disease spondyloepiphyseal dysplasia tarda. *J. Biol. Chem.* **277**, 49863–49869 (2002).
34. Dietrich, L.E., Gurezka, R., Veit, M. & Ungermann, C. The SNARE Ykt6 mediates protein palmitoylation during an early stage of homotypic vacuole fusion. *EMBO J.* **23**, 45–53 (2004).
35. Terwilliger, T.C. & Berendzen, J. Automated MAD and MIR structure solution. *Acta Crystallogr. D* **55**, 849–861 (1999).
36. Terwilliger, T.C. Maximum-likelihood density modification. *Acta Crystallogr. D* **56**, 965–972 (2000).
37. Jones, T.A., Zou, J.Y., Cowan, S.W. & Kjeldgaard, M. Improved methods for binding protein models in electron density maps and the location of errors in these models. *Acta Crystallogr. A* **47**, 110–119 (1991).
38. Brunger, A.T. *et al.* Crystallography & NMR system: A new software suite for macromolecular structure determination. *Acta Crystallogr. D* **54**, 905–921 (1998).
39. Otwinowski, Z. & Minor, W. Processing of X-ray diffraction data collected in oscillation mode. *Methods Enzymol.* **276**, 307–326 (1997).
40. Collaborative Computational Project, Number 4. The CCP4 suite: programs for protein crystallography. *Acta Crystallogr. D* **50**, 760–763 (1994).
41. Thompson, J.D., Higgins, D.G. & Gibson, T.J. CLUSTAL W: improving the sensitivity of progressive multiple sequence alignment through sequence weighting, position-specific gap penalties and weight matrix choice. *Nucleic Acids Res.* **22**, 4673–4680 (1994).